Coexistence of strong 3*d* antiferromagnetism and mixed-valent Kondo regime transition in $Ce(Mn_xCr_{1-x})_2Si_2$

G. Liang and M. Croft
Department of Physics and Astronomy, Rutgers University, Piscataway, New Jersey 08855-0849

D. C. Johnston*
Exxon Research and Engineering Company, Route 22 East, Annandale, New Jersey 08801

N. Anbalagan and T. Mihalisin
Department of Physics, Temple University, Philadelphia, Pennsylvania 19122
(Received 7 April 1988)

Structural, thermal, magnetic, transport, and Ce L_3-edge spectroscopic measurements on the $Ce(Mn_xCr_{1-x})_2Si_2$ series are presented. These results all indicate that Cr substitution drives this system from a mixed-valent Ce state at $x=1.0$ to a Kondo or heavy-fermion state with increasing x. The reflection of the Ce valence-state variation (from L_3 measurements) in the electronic specific heat coefficient and lattice parameters is discussed. The magnetic and transport measurements indicate that the Ce spin-flip scattering processes (i.e., the Kondo effect) apparently thrive within the Mn-moment antiferromagnetically ordered phase of these compounds.

I. INTRODUCTION

Recently, the $ThCr_2Si_2$-structure compounds CeT_2Si_2 have been shown to exhibit an evolution from a Kondo regime for $T=$Cu to a mixed-valent (MV) regime for $T=$Ni, Co, Fe, and Mn followed by a reentrance into a Kondo regime between $T=$Mn and Cr.[1] It is important to note that the Mn atoms in $CeMn_2Si_2$ exhibit antiferromagnetic order at $T_N=376$ K in $CeMn_2Si_2$ despite the MV state for Ce in this compound.[2] Thus the $Ce(Mn_{1-x}Cr_x)_2Si_2$ system offers the opportunity to study the Ce MV to Kondo regime passage in a host where strong 3*d* magnetism could interplay with this passage. Specifically, internal or external magnetic fields with energy scales much larger than the Ce spin-fluctuation temperature might be expected to quench the nonmagnetic MV or Kondo behavior. As we shall see, however, in many respects, the Ce MV and Kondo effects appear to coexist (indeed to thrive) between the antiferromagnetically ordered Mn sublattices in this material.

A second important point which should be noted while reading this paper is the continuous way in which the Kondo regime evolves out of the MV regime. This is consistent with the idea that the MV and Kondo regimes (for Ce at least) are, respectively, the high-energy scale spin-fluctuation and low-energy scale spin-fluctuation regimes of the same problem. Indeed the thermal Ce L_3 valence variations observed here appear consistent with recent Anderson model treatments by Schlottmann[3] and Bickers *et al.*[4] and Rice *et al.*[5]

II. EXPERIMENT

The polycrystalline sample preparation and resisitivity measurement methods have been discussed previously.[1] The susceptibility and resistivity samples were (in almost all cases) taken from the same master samples. The much more massive specific heat samples were prepared separately. The specific heat and L_3 measurement and analysis methods have been described elsewhere.[6,7] The susceptibility measurements were made with a Faraday magnetometer in a magnetic field (H) of 6.3 kOe. Ferromagnetic impurity contributions have been corrected for via separate magnetization M versus H isotherms at several temperatures.

The x-ray diffraction data were taken at room temperature on an automated diffractometer. The lattice parameters were obtained by the least-squares-fitting method in the range of $20° \le 2\theta < 80°$. X-ray diffraction indicated that all of the samples were single phase with $ThCr_2Si_2$ crystal structure except two specific heat samples with $x=0.8$ and 0.7, which showed a weak second $CeSi_x$ ($x=1.7-2.0$) phase presumably due to the Mn mass loss.

III. RESULTS AND DISCUSSION

A. Lattice-parameter results

The lattice parameters and cell volume (as determined by x-ray diffraction studies) for the $Ce(Mn,Cr)_2Si_2$ series are plotted versus x in Fig. 1(a). The first points we wish to note are that both the a-parameter and cell-volume (V) data exhibit a nearly linear x dependence (i.e., Vegard's-law behavior) for $0.2 \le x \le 0.7$, and that both a and V show a strong compressive deviation from this linear behavior onsetting and growing continuously between $x=0.7$ and $x=1.0$. The c-axis parameter remains much closer to a Vegard's-law-type behavior with a small compressive effect (similar to the a and V results) occurring for $x > 0.7$.

Association of these a and V compressions with an anomalous Ce-atom radius contraction (at 300 K) be-

tween $x=0.7$ and $x=1.0$ is supported by two things. First is the observation that the a and V parameters of the 1:2:2 compound series typically respond to the lanthanide contraction but the c parameter typically does not. Second is the observation that the a and V parameters of $EuPd_2Si_2$ respond directly to the nonlinear Eu valence (atomic radius) change but the c parameter does not.[8,9]

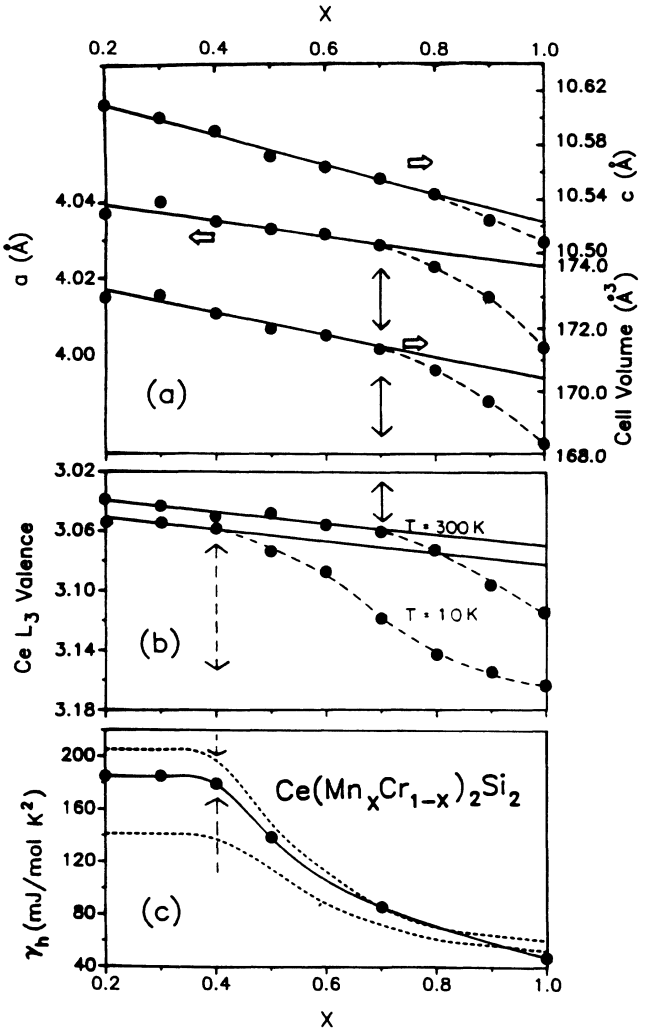

FIG. 1. $Ce(Mn_xCr_{1-x})_2Si_2$ series results as a function of x for (a) the a and c parameters and unit-cell volume V; (b) the Ce L_3 valence v_3 at $T=300$ and 10 K; (c) the "high-temperature" ($T\sim 10$ K) linear coefficient of the specific heat γ_h. The solid and dashed lines in (a) and (b) guide the eye, respectively, through the linear and nonlinear data variations. The arrows are included to emphasize the close agreement of the room-temperature lattice and L_3 results and of the 10 K γ_h and L_3 results. Finally in (c) the dashed curves represent the relation $\gamma=\gamma_0/(v-3)$ with $\gamma_0=9$ mJ/mol K^2. Here the two dashed curves were generated from our 10 K L_3 results (v_3). The values of the valence v substituted into this formula were $v_3\pm 0.01$ thereby generating the two dashed curves reflecting the role of experimental uncertainty in the specific heat γ prediction from the L_3 valence data.

B. L_3 x-ray absorption spectroscopy: general remarks

L_3-edge x-ray absorption spectroscopy (XAS) has been proved to be a very valuable tool in determining the valence in the mixed-valence field.[7,10–13] The large number of unoccupied $5d$ orbitals in rare-earth atoms produces (via $2p\rightarrow 5d$ transition) a prominent peak (the so-called L_3 white line) just above the L_3 absorption edge. In addition, an arctangent-type step-function feature, due to $2p_{3/2}\rightarrow$continuum transitions, occurs at the L_3 edge. In rare-earth materials, the removal of an electron from the $4f$ shell (e.g., $Ce^{3+}\,4f^1\rightarrow Ce^{4+}\,4f^0$) reduces the screening of the $2p$ orbital thereby shifting the $2p_{3/2}$ energy level down by approximately 7–10 eV. A mixed-valent atom executes a quantum tunneling between two $4f$ level occupation states (valence states) on a time scale ($\sim 10^{-13}$ sec) which is slow compared to the L_3 XAS time scale (10^{-17} sec). Thus the L_3 edge of a MV atom consists of a superposition of two integral valent edges separated by 7–10 eV. The weight of each valence state in the MV state is evaluated by determining the spectral weight of the two integral valent edge features required to model the spectrum.

In Fig. 2 (top) we illustrate these ideas by showing the separate Ce^{3+} and Ce^{4+} components used to model the

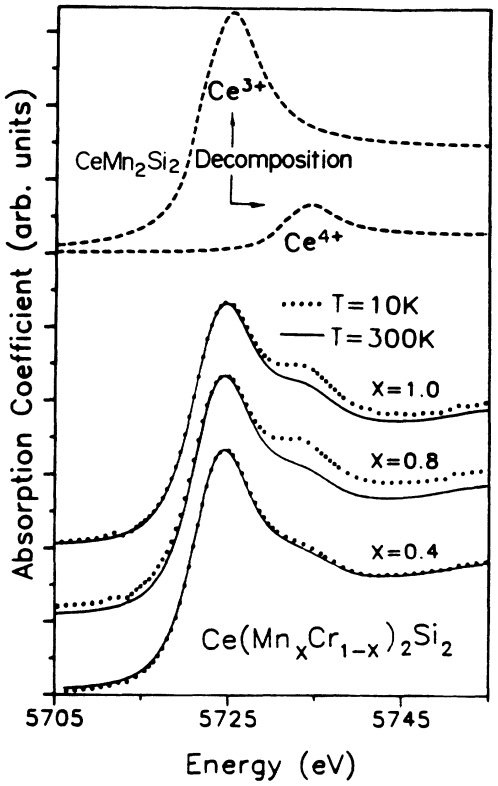

FIG. 2. Ce L_3 spectra, all normalized to the Ce^{3+} peak, at $T=10$ K (dotted curves) and room temperature (solid curves) for three selected $Ce(Mn_xCr_{1-x})_2Si_2$ compounds. At the top of the figure, the separated Ce^{3+} and Ce^{4+} contributions to the Ce L_3 edge of $CeMn_2Si_2$ at $T=10$ K ($v_3=3.16$), as determined by our fitting procedure, are shown.

Ce L_3 spectrum of $CeMn_2Si_2$ ($T=10$ K) (pictured in the same figure). The details of the fitting procedure have been discussed elsewhere.[7] The derived L_3 valence value (v_3) for this material is $v_3=3.16$. Whether the L_3 valence is in fact the absolute valence for Ce compounds is at present an unanswered question. However, in many Ce systems a one-to-one correspondence has been established between the Ce-volume collapse (associated with Ce valence mixing) and the Ce L_3 valence change. The spirit in which we use the L_3-valence values therefore is to identify *changes* in the Ce valence state.

We display the experimental Ce L_3 spectra superimposed and normalized to the first (Ce^{3+} related) peak. With this normalization and superposition procedure, a spectrum with a higher v_3 value will lie naturally above a spectrum with a lower v_3 value in the energy range of the second (Ce^{4+} related) peak. In this way a fitting-procedure-independent picture of the spectral evolution evidencing a Ce valence change can be seen.

C. L_3 results at room temperature

Our L_3 XAS results motivate a number of conclusions. See Fig. 1(b) for the v_3 variation versus x and Figs. 3 for the spectra. First, the Ce L_3 valence (v_3) at $x=1.0$ is 3.12, typical of a mixed-valent material like $CePd_3$, and with Cr substitution v_3 is decreased continuously to 3.04 (at $x=0.2$), typical of a Kondo regime material like $CeCu_2Si_2$.[1,7] Second, the anomalous compressions in the a- and V-parameter results, noted above, track the v_3 results quite closely. That is, there appears to be a much more rapid change in v_3 between $x=0.8$ and 1.0 which is reflected in a one-to-one way by the lattice-parameter results.

In previous work, we have nominally associated v_3 values in the 3.07–3.10 range (at room temperature) as indicating the borderline between MV regime behavior (for larger v_3 values) and Kondo regime behavior (for smaller v_3 values).[1] Here the lower end of this borderline occurs near $x=0.8$, above which v_3 and the lattice parameters manifest stronger x variations. The resistivity results presented later also appear to support the passage into the Kondo regime (i.e., lower-energy scale spin fluctuations) somewhere in this same range. However, it should be noted that some variation in v_3 persists for $x \lesssim 0.8$ in the Kondo regime. This is in line with theoretical Anderson model results in which spin-fluctuation energy scale and small Ce valence variations go hand in hand.[3–5] The low-temperature v_3 values discussed below further underscore the continuity of the physics underlying the MV to Kondo regime passage.

D. L_3 results at 10 K

Mixed-valent materials typically show valence variations below room temperature. In Fig. 1(b) we show the v_3 values for the $Ce(Mn,Cr)_2Si_2$ series at 10 K (see Fig. 2 for illustrative spectra). These data exhibit the following features: (1) Ce L_3 valence increases in general with decreasing temperature; (2) the Ce L_3 valence shows little temperature-induced change for the nearly trivalent compounds ($x<0.4$); and (3) for $x>0.4$ the thermal valence variation grows continuously to a rather substantial value at $x=1.0$.

The observed thermal variation of the v_3 (and therefore the $4f$ occupation number n_f) is consistent with the degenerate Anderson model calculations by Schlottmann[3] and the recent self-consistent large-N-expansion calculations by Bickers *et al.*[4] Their work showed[4] thermal n_f decreases (i.e., valence increases) on the same order as the v_3 variations we observe [i.e., $\Delta v_3 = v_3(10\text{ K}) - v_3(300\text{ K}) \lesssim 0.08e^-$].

E. Specific heat results

We now turn to the low-temperature specific heat result on the $Ce(Mn_xCr_{1-x})_2Si_2$ series. The values of the linear coefficient of the specific heat, γ, were obtained from the data by fitting to the relation $C/T=\gamma+\beta T^2$ in the range of T from 10 to 25 K. We observed a small bump at $T\approx 6$ K for the entire series, similar to that attributed in the MV compound $CePd_3$ to Ce_2O_3 impurities.[6,14] The estimated entropy due to this bump is about 25 mJ/mol K corresponding to about 0.4% of the Ce atoms in our compounds if we attribute it to the magnetic phase transition of the Ce_2O_3 impurities. We also observed a second small bump for $x=0.2$–0.5 at $T\sim 7.4$–9.9 K. This bump is due to the very weak $CeSi_y$ ($1.7<y<2.0$) phase. The $CeSi_y$ impurities constitute less than 5% of the Ce atoms by entropy estimate for $x=0.2$ and 0.3, and less than 1% for $x=0.4$ and 0.5.

Heavy-fermion systems typically show a very strong increase in their γ values below 10 K and in some cases below 1 K.[15] For $CeCu_2Si_2$ at roughly 10, 4, and 1 K the γ values are, respectively, ~110, 180, and 1050

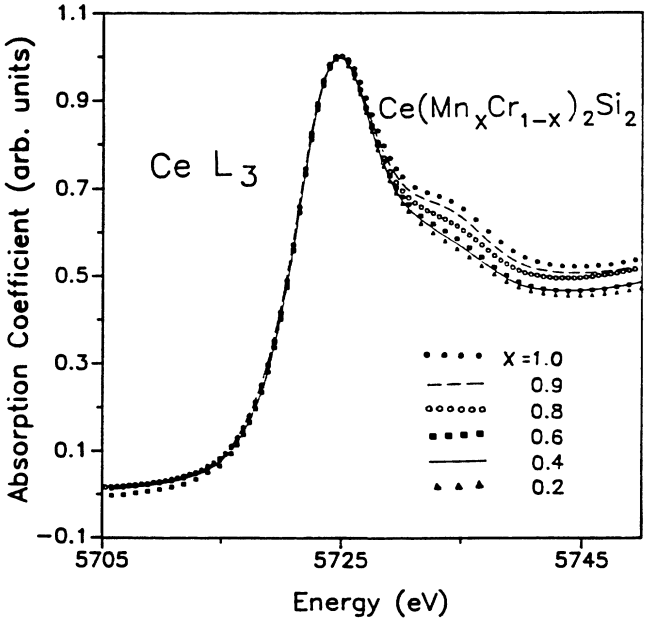

FIG. 3. Ce L_3 absorption spectra of $Ce(Mn_xCr_{1-x})_2Si_2$ compounds superimposed to compare intensity in the Ce peak region, all normalized to the Ce^{3+} peak.

mJ/mol K^2, respectively.[16] Since we are using the γ values from fitting data in the 10–25-K range we will refer to our results as γ_h for "higher-temperature" linear specific coefficient. In mixed-valent materials where γ typically has little thermal variation below 10 K no distinction between the $T=0$ and high-temperature γ values need be made.

The γ_h value is 47 mJ/mol K^2 for $CeMn_2Si_2$, analogous to that of typical MV compounds (e.g., for $CePd_3$, $\gamma \sim 38$ mJ/mol K^2). The γ_h values increase dramatically as one moves towards the nearly trivalent Kondo regime until at $x=0.2$, $\gamma_h = 184.7$ mJ/mol K^2 [see Fig. 1(c)]. Such a value of γ_h is typical of a Kondo regime or heavy-fermion system. By comparison the γ_h values for the heavy-fermion system $CeCu_2Si_2$ and the Kondo system $Ce(Pd_{0.87}Ag_{0.13})_3$ are both[6] well under 200 mJ/mol K^2. As will be noted in the next section, the enhancement of γ in Kondo-MV systems is associated with the increase in the f-quasiparticle density of states at ε_F which has a width proportional to T_{SF} (the spin-fluctuation or Kondo temperature) and a height proportional to $1/T_{SF}$. Thus the γ enhancement is associated with a decrease in T_{SF}.[16]

F. γ_h-v_3 correlation

It is important to note that the γ_h values versus x data correlate very closely with the 10-K L_3 valence variation data [Fig. 1(b)]. That is, the γ_h values become independent of x where the thermal variation of v_3 nearly disappears (i.e., for $x \lesssim 0.4$); and the γ_h and v_3 data both show strong variations with x between $x=0.4$ and $x=1.0$. We would like to underscore that the L_3 valence at 10 K is thus supported by the ground-state measurements (specific heat) as the 300-K L_3 valence variation was supported by the ground-state lattice-parameter measurements. As noted earlier, this supports our claim that L_3 valence variations (i.e., Δv_3) faithfully reflect (but are not necessarily equal to) the absolute valence variations (i.e., Δv). Although the scaling between Δv_3 and Δv may be nonlinear in the absence of evidence to the contrary we would propose $\Delta v_3 \sim \Delta v$.

From a theoretical viewpoint, the similar x variations of γ_h and v_3 appear to be reasonable. Increasing Cr substitution should be acting to decrease the spin-fluctuation or Kondo temperature (T_{SF}). (This will be supported by our transport results discussed below.) The notion that the f-related quasiparticle density of states at the Fermi energy scales with $1/T_{SF}$ or that $\gamma \sim 1/T_{SF}$ is a long-standing one in the mixed-valent–heavy-fermion field.[17] Rice *et al.*[5] have recently pointed out that one also expects the effective mass $m^* \sim T_{SF}^{-1} \sim \gamma(1-n_f)^{-1}$ where n_f is the Ce $4f$ occupation number. Thus, since the absolute valence $v=4-n_f$, one would in general expect variations in n_f to lead to variations in both γ and v_3.

If one makes the assumption that the L_3 valence (v_3) actually yields the absolute valence one can be somewhat more quantitative. (Recall that we have indicated that we regard this as a trial ansatz only.) With this assumption, one can use $n_f = 4 - v_3$ to extract n_f values from our v_3 data and $\gamma = \gamma_0(1-n_f)^{-1}$ to derive the corresponding specific heat values from our v_3 results. The dashed lines in Fig. 1(c) represent the results of this procedure with $\gamma_0 = 9$ mJ/mol K^2 and an optimistic uncertainty in v_3 of ± 0.01. This quantitative agreement is interesting, however we only wish to use it (at present) to stress the natural correlation between the v_3 (10 K) and the specific heat γ_h results.

G. Magnetic susceptibility and magnetism

Shown in Fig. 4 is the thermal dependence of the magnetic susceptibility $\chi(T)$ for four samples in the $Ce(Mn,Cr)_2Si_2$ system. All of the samples, except for $x=0.2$, evidence antiferromagnetic ordering at Néel temperatures (T_N) which (together with the paramagnetic Curie-Weiss temperature Θ, effective moment μ_{eff} and the saturation moment μ_{sat}) are listed in Table I. For the $x=0.2$ sample, paramagnetic behavior was found in the entire temperature range. The Θ and μ_{eff} values were obtained by fitting the data to a Curie-Weiss law $\chi = C/(T-\Theta)+\chi_0$ on the high-temperature (paramagnetic) side of the $\chi(T)$ peaks. The antiferromagnetic nature of the ordering in all samples was supported by the precursors of the so-called "spin-flop" transition observed in high-field magnetization measurements at several temperatures below T_N (the M-versus-H plots are not shown here). No evidence for Ce magnetic ordering was detected in this series. We are currently pursuing low-field and ac magnetic measurements to probe for possible short-range order or spin-glass effects in samples with low Mn content.

It has been previously reported that no magnetic moments are detected on the Ce atoms in $CeMn_2Si_2$ by neutron scattering,[18] which is consistent with the observation that $CeMn_2Si_2$ is a MV system. The upturn of the $\chi(T)$ below 50 K (see Fig. 4) could contain contributions from both the standard paramagnetic impurities and possibly the low T_{SF} impurity sites for the Ce atoms. It would ap-

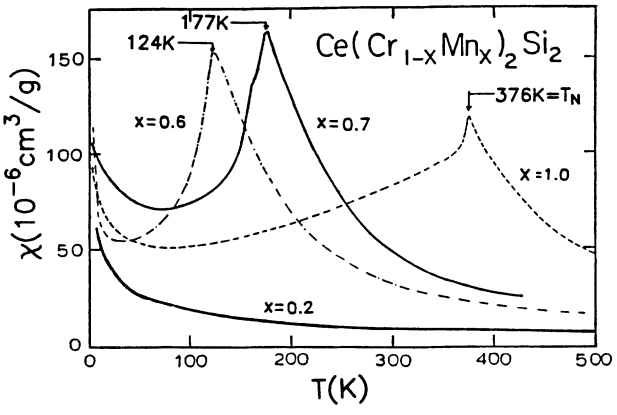

FIG. 4. Temperature dependence of the magnetic susceptibility $\chi(T)$ of the $Ce(Mn_xCr_{1-x})_2Si_2$ series. Note the sharp peaks in the susceptibility (except for $x=0.2$ sample) near the antiferromagnetic ordering temperatures T_N. Note also the decrease of T_N with decreasing x.

TABLE I. Magnetic susceptibility data for $Ce(Mn_xCr_{1-x})_2Si_2$ compounds determined from χ-vs-T measurements.

Compounds	T_N (K)	Θ (K)	μ_{eff} (units of μ_B)	μ_{sat} (units of μ_B)
$CeMn_2Si_2$	376	319	3.28	2.42
$Ce(Mn_{0.7}Cr_{0.3})_2Si_2$	177	165	3.38	2.52
$Ce(Mn_{0.6}Cr_{0.4})_2Si_2$	124	145	2.92	2.09
$Ce(Mn_{0.2}Cr_{0.8})_2Si_2$		−66	3.73	2.86

pear reasonable to propose that the magnetic structure in the $Ce(Mn_xCr_{1-x})_2Si_2$ series is similar to that of $CeMn_2Si_2$. That is, with ferromagnetically ordered Mn-Cr layers in the a planes which are antiferromagnetically aligned along the c axis and with the nonmagnetic Ce and Si layers lying in between.[18] The ferromagneticlike Θ values for these ordered compounds (like in $CeMn_2Si_2$) support this proposal.

The T_N values were found to decrease linearly with x at a rate of $\Delta T_N/\Delta x \sim 6.0$ K/(at.% Mn) for the $Ce(Mn_xCr_{1-x})_2Si_2$ series. The fact that Obermeyre *et al.*[19] have observed a very similar linear rate of depression of T_N [i.e., 6.3 K/(at.% Mn)] in the $Nd(Mn_xCr_{1-x})_2Si_2$ system supports the notion that the rare-earth sublattice plays very little role in the high-temperature ordering in these alloys. In Fig. 5 we plot T_N against x along with literature results for the $Ce(Fe_{1-y}Mn_y)_2Si_2$ system.[20] We attribute the sharp drop of T_N to dilution and the breakup of percolation in the ferromagnetic Mn planes through the weakly magnetic

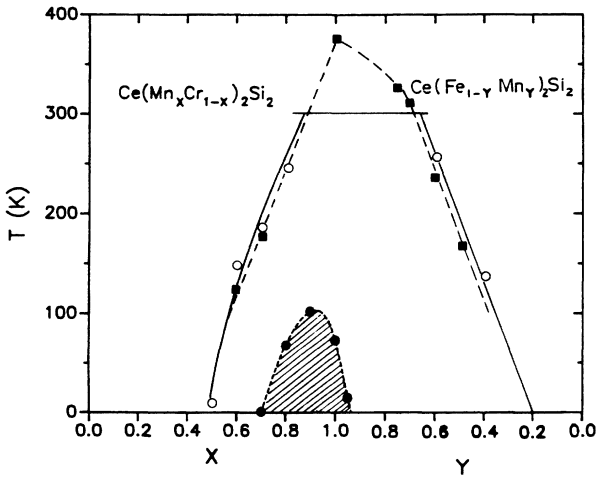

FIG. 5. The Néel temperature T_N (solid squares connected by dashed lines), resistivity minimum temperature T_{min} (open circles and connected by solid lines), and resistivity maximum temperature T_{max} (solid circles) vs manganese concentrations x and y for $Ce(Mn_xCr_{1-x})_2Si_2$ and $Ce(Fe_{1-y}Mn_y)_2Si_2$ series. The shaded area at low temperature is the region related to coherent scattering between Ce sites. The dashed curves and solid curves are guides to the eye. Note the close correlation between T_N and T_{min} for both the Cr and Fe substituted series. The T_N data are from both our work and Ref. 20.

Cr and Fe substitution. Thus, Figs. 4 and 5 show that there is an antiferromagnetic to paramagnetic evolution as x is decreased from $x=1.0$ to $x=0.2$ in $Ce(Mn_xCr_{1-x})_2Si_2$.

The large $3d$ interlayer distance (equal to $c/2 \sim 5.3$ Å) in the $Ce(Mn_xCr_{1-x})_2Si_2$ compounds and the Ce-Si-Mn(Cr)-Si-Ce layer structure suggest that indirect interaction is responsible for the interlayer $3d$ antiferromagnetic ordering. Although some authors[21] attribute the interlayer interactions to superexchange the metallic character of these compounds would suggest Ruderman-Kittel-Kasuya-Yosida (RKKY) interactions mediated via the conduction electrons.

The effective moment of Mn in $CeMn_2Si_2$ is $\mu_{eff}=3.28\mu_B$, much smaller than the $5.9\mu_B$ of the $Mn^{5+}(3d^5)$ ions. Within a formal Mn local moment interpretation these values correspond to a combination of 45% $3d^7$ and 55% $3d^8$ per Mn atom. Recently, Szytula *et al.*[21] have proposed that the short Mn-Si distance (2.4 Å) in this compound makes it possible for the electronic charge to transfer from the $3p$ shell of Si to the $3d$ shell of Mn, thereby achieving the requisite d-orbital charge increase. Of course, interactions of the Mn $3d$ states with itinearant band states could also lead to Mn moment reduction with smaller d-orbital occupation changes. The $\mu_{eff}=3.73\mu_B$ for $Ce(Mn_{0.2}Cr_{0.8})_2Si_2$ is $0.45\mu_B$ larger than that for $CeMn_2Si_2$. This could reflect the Ce moment formation (as might be expected) in the nearly trivalent Ce end of the $Ce(Mn,Cr)_2Si_2$ series.

H. Resistivity results

We show in Fig. 6 the resistivity $\rho(T)$ of the $Ce(Mn_xCr_{1-x})_2Si_2$ (the Ce series) from 1.7 K to room temperature after subtracting the $\rho(T)$ of $Th(Mn_xCr_{1-x})_2Si_2$ (the Th series). Here the Th-series $\rho(T)$ measurements were used to estimate both the Mn magnetic and phonon background scattering. We chose this Th series rather than the $La(Mn_xCr_{1-x})_2Si_2$ series to estimate the $\rho(T)$ background based on their magnetic structure. That is, $ThMn_2Si_2$ has the same antiferromagnetic structure[21] ($T_N=483$ K) as $CeMn_2Si_2$, while $LaMn_2Si_2$, on the other hand, orders ferromagnetically at 303 K.[21]

The basic feature of the $\rho(T)$ curves of the $Th(Mn_xCr_{1-x})Si_2$ compounds (which are not shown here) is a phononlike behavior except for the $x=0.5$ and 0.6 samples which exhibited a wide but small amplitude bump at about 120 and 160 K, respectively. We illustrate

the Ce- and Th-system resistivities for the $x=0.8$ in the inset of Fig. 6. The absolute value of $\rho(T)$ for the Th series was always smaller than that of the corresponding Ce compounds.

It is clear in Fig. 6 that the temperature dependence of the resistivity of the background-subtracted $Ce(Mn_xCr_{1-x})_2Si_2$ series is very similar to the $\rho(T)$ plotted in Ref. 1 where no background was subtracted. That is, (1) the MV compound $CeMn_2Si_2$ displays a high-T negative temperature coefficient of resistivity (TCR) along with a rapid low-T resistivity drop from a maximum at $T=73$ K [this $\rho(T)$ feature is very similar to what was found in the prototypic MV system $CePd_3$, and is related to the onset of coherent scattering between different Ce sites]; (2) with x moving down from $x=1$, this coherency effect is rapidly destroyed by the disorder of the Mn-Cr sublattice and almost disappears by $x=0.8$; and (3) the positions of the low-temperature minimum (T_{min}) are almost unchanged by the background subtraction. The T_{min} values move down steadily with decreasing Mn content and, as will be emphasized below, are closely correlated with the onset of the antiferromagnetic ordering of the 3d sublattice. Thus the anomalous increases in the $\rho(T)$ curves, with decreasing temperature, can be attributed to Ce scattering, presumably of Kondo-spin-flip type. The negative curvature of $\rho(T)$ which develops for $x \leq 0.5$ is very similar to that found in some Kondo systems such as $CeAl_3$,[22] where they have been interpreted in terms of a Kondo modified crystalline electrical field effect as treated by Cornut and Coqblin.[23]

The Kondolike resistivities in this series occur at progressively lower temperature ranges and become weaker with increase in Cr content. This is consistent with the evolution from MV to Kondo regimes and decreasing spin-fluctuation temperatures evidenced in the earlier lattice parameters—L_3, specific heat, and magnetic susceptibility results.

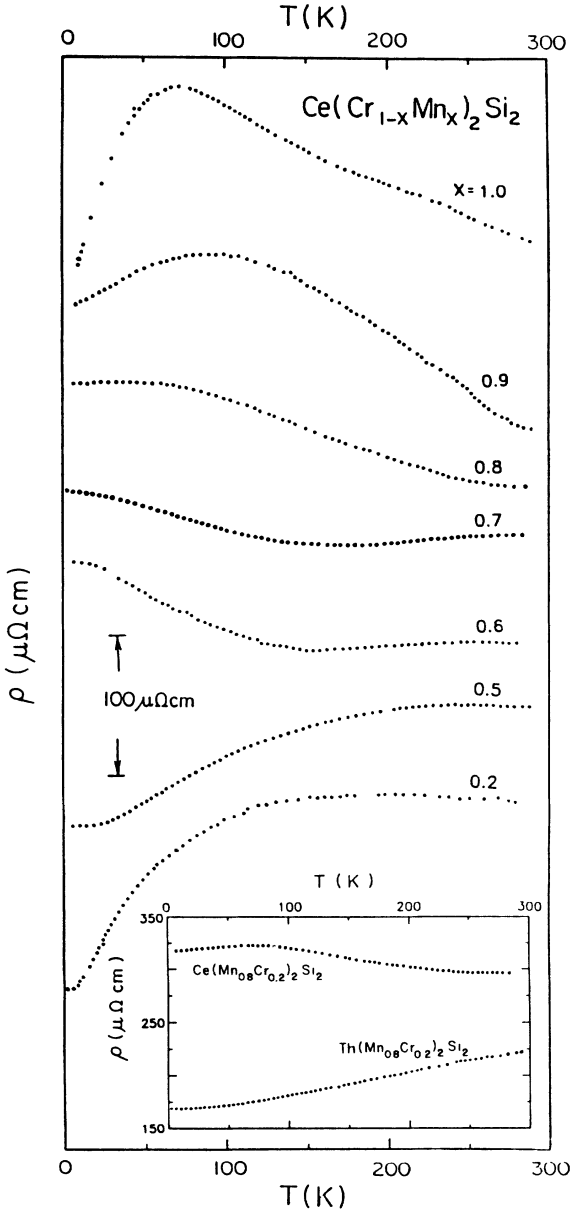

FIG. 6. Electrical resistivity vs temperature results for the $Ce(Mn_xCr_{1-x})_2Si_2$ series after subtracting the $Th(Mn_xCr_{1-x})_2Si_2$ background, i.e., the Mn magnetic and phonon background scattering. The inset shows the resistivity for the $x=0.8$ compounds. Note the rapid quenching of the low-temperature coherence and the steady state decrease of the resistivity minimum temperature as x moves down from $x=1.0$.

I. Antiferromagnetic-order–Kondo-scattering correlation

We would now like to discuss the correlation of the Kondo minimum temperature T_{min} to the 3d antiferromagnetic ordering temperature T_N. We have observed that the T_{min} values of the $\rho(T)$ curves are very close to the T_N values for the $Ce(Mn_xCr_{1-x})_2Si_2$ series (see Fig. 5). The small deviation of T_N from T_{min} for $x=0.6$ can reasonably be considered within measurement and sample duplication errors. Recently, we have also observed this T_N and T_{min} correlation in the $CeMn_2(Si_xGe_{1-x})_2$

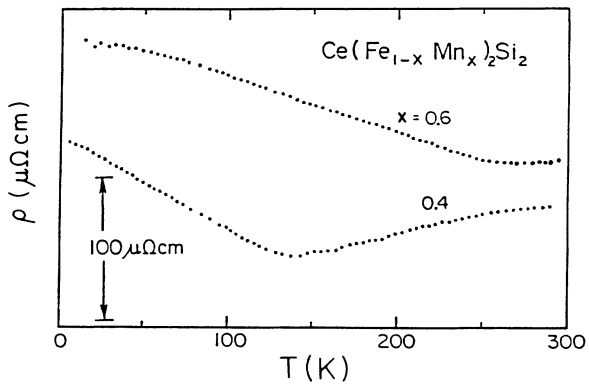

FIG. 7. Electrical resistivity vs temperature results for two $Ce(Fe_{1-y}Mn_y)_2Si_2$ compounds after subtracting the corresponding background, i.e., the resisitivity of $Th(Fe_{1-y}Mn_y)_2Si_2$. Note the resistivity minimum at temperature close to T_N (see Fig. 5).

series.[24]

This closeness of T_N and T_{min} can potentially be explained by the effect of the 3*d* magnetic field on the Ce atoms in the following picture. Above T_N the Ce spins are actually acted on by a local time varying RKKY field (or conduction electron polarization field), produced by the Mn moments which are in the nearest-neighbor layers.[25] In this case the Ce Kondo spin-flip process could be effectively quenched by this dynamic RKKY field. When the temperature falls below T_N, the interlayer 3*d* antiferromagnetic ordering occurs giving rise to a static RKKY field. The resulting static RKKY field could be much smaller at the Ce sites which are symmetrically located between oppositely aligned ferromagnetic 3*d* (Mn-Cr) layers. Thus, the Kondo spin-flip process could be freed up below T_N and the Kondo-type negative TCR would arise at a temperature near T_N. If the 3*d* sublattices were ferromagnetically ordered then the Ce Kondo spin-flip processes would presumably be further quenched by a large static RKKY field and thus no resistivity minimum would be expected.

Further evidence of the onset of Ce scattering in the antiferromagnetic phase of these types of compounds can be gleaned from the background-subtracted resistivity, $\rho(T)$, curves of the $Ce(Fe_{1-y}Mn_y)_2Si_2$ shown in Fig. 7. A resistivity minimum occurs at ~ 2.52 and 138 K for $x=0.6$ and 0.4, respectively, in this system. These values are very close to the T_N value observed by Sztula *et al.*[20] (see Fig. 5). The $Ce(Mn,Fe)_2Si_2$ samples are within the MV regime. However, the disordered MV materials (such as $CePd_3$ or $CeMn_2Si_2$) have been shown to exhibit a negative TCR reminiscent of the Kondo effect. Thus, in this system, also the Ce scattering appears quenched above T_N but freed up below T_N.

IV. SUMMARY

In summary, we have found $Ce(Mn_xCr_{1-x})_2Si_2$, with $0.2 \leq x \leq 1.0$, to be the first compound series in which the Ce undergoes an evolution from a coherent MV regime to a noncoherent nearly trivalent Kondo system despite the presence of strongly interacting 3*d* moments. Indeed, the continuous nature of this evolution appears consistent with the philosophy of recent Anderson-model treatments[3-5] in which the 4*f* occupancy varies in the $1.0 \geq n_f \geq 0.7$ range. More specifically, some of the noteworthy points that have been brought out are listed below.

(1) Ce Kondo-type spin-fluctuation scattering apparently thrives within the antiferromagnetically ordered phase of these materials.

(2) The paramagnetic state of these materials containing Mn moments appears hostile to the Ce spin-flip (i.e., Kondo scattering) process.

(3) the Ce L_3 valence variation and lattice parameter results at 300 K both support a Ce valence decrease with Cr substitution in these materials.

(4) The enhancement of the low-temperature specific heat with Cr substitution is consistent in magnitude with the observed Ce L_3 valence state variation (at 10 K) in the light of recent theoretical work.[3-5]

Finally, our work should motivate generalizations of traditional Anderson-model treatments of MV-Kondo phenomena to magnetic host lattices. Specifically, the band states with which the 4*f* states hybridize could be considered to be partially spin polarized in a static or dynamic way. Questions also arise of how the band electron RKKY field interacts spatially with the Ce 4*f* moment screening cloud set up in the Kondo ground state.

*Present address: Physics Department and Ames Laboratory (U.S. DOE), Iowa State University, Ames, Iowa 50011.

[1]G. Liang, M. Croft, R. Neifeld, and B. Qi, J. Appl. Phys. **61**, 3181 (1987), and references therein.

[2]G. Liang, M. Croft, D. C. Johnston, N. Anbalagan, and T. Mihalisin, Phys. Rev. B **37**, 5970 (1988).

[3]P. Schlottmann, Z. Phys. B **56**, 127 (1984).

[4]N. E. Bickers, D. L. Cox, and J. W. Wilkins, Phys. Rev. B **36**, 2036 (1987).

[5]T. M. Rice and K. Ueda, Phys. Rev. B **34**, 6420 (1986).

[6]T. Mihalisin, P. Scoboria, and J. A. Ward, Phys. Rev. Lett. **46**, 862 (1981).

[7]M. Croft, R. Neifeld, C. U. Segre, S. Raaen, and R. D. Parks, Phys. Rev. B **30**, 4164 (1984).

[8]E. Kemly, M. Croft, V. Murgai, L. C. Gupta, C. Godart, R. D. Parks, and C. U. Segre, J. Magn. Magn. Mater. **47&48**, 403 (1985).

[9]E. V. Sampathkumaran, R. Vijayaraghavan, K. V. Gopalakrishnan, R. G. Pilley, H. G. Devare, L. C. Gupta, Ben Post, and R. D. Parks, in *Valence Fluctuations in Solids*, edited by L. M. Falicov, W. Hanke, and M. B. Maple (North-Holland, New York, 1981), p. 93.

[10]R. A. Neifeld, M. Croft, T. Mihalisin, C. U. Segre, M. Madigan, M. S. Torikachvili, M. B. Maple, and L. E. Delong, Phys. Rev. B **32**, 6928 (1985).

[11]K. P. Bauchspiess, W. Boksch, E. Holland-Moritz, H. Launois, R. Pott, and D. Wohlleben, in *Valence Fluctuations in Solids*, Ref. 9, p. 417.

[12]R. D. Parks, S. Raaen, M. L. den Boer, V. Murgai, and T. Mihalisin, Phys. Rev. B **28**, 3556 (1983).

[13]P. Weidner, K. Keulerz, R. Lohe, B. Roden, J. Rohler, B. Wittershagen, and D. Wohlleben, J. Magn. Magn. Mater. **47&48**, 75 (1985).

[14]M. J. Besnus, J. P. Kappler, and A. Meyer, J. Phys. F **13**, 5971 (1983).

[15]G. R. Stewart, Rev. Mod. Phys. **56**, 755 (1984).

[16]G. R. Stewart, Z. Fisk, and J. P. Willis, Phys. Rev. **28**, 172 (1983); N. B. Brandt and V. V. Moshchulkov, Adv. Phys. **33**, 373 (1984).

[17]D. M. Newns, A. C. Hewson, J. W. Rasul, and N. Read, J. Appl. Phys. **53**, 7877 (1982).

[18]S. Siek, A. Szytula, and J. Leciejewicz, Phys. Status Solidi A **46**, K101 (1978).

[19]R. Obermyer, S. G. Sankar, and V. U. S. Rao, J. Appl. Phys. **50**, 2312 (1979).

[20]A. Szytula and S. Siek (unpublished).

[21]A. Szytula and S. Siek, J. Magn. Mater. **27**, 49 (1982); Z. Ban, L. Omejec, A. Szytula, and Z. Tomkowick, Phys. Status Solidi A **27**, 333 (1975).
[22]A. Percheron, J. C. Achard, O. Gorochov, B. Cornut, D. Terome, and B. Coqblin, Solid State Commun. **12**, 1289 (1973).
[23]B. Cornut and B. Coqblin, Phys. Rev. B **5**, 4541 (1972).
[24]G. Liang and M. Croft (unpublished).
[25]J. Hubbard, J. Appl. Phys. **52**, 1654 (1981).